Aging and Disease
www.aginganddisease.org
Early access date: February 26, 2025
http://dx.doi.org/10.14336/AD.2024.1430

Original Article

Trifluoroacetic Acid Induced a Cyclophilin D-Dependent Cognitive Impairment in Mice

Yun Li[1,2#], Yichi Xu[1,3], Yuanlin Dong[1], Christa J. Nehs[4], Zhongcong Xie[1], Yiying Zhang[1*]

[1]Geriatric Anesthesia Research Unit, Department of Anesthesia, Critical Care and Pain Medicine, Massachusetts General Hospital and Harvard Medical School, Charlestown, MA 02129, USA. [2]Department of Anesthesia, Beijing Tiantan Hospital, Capital Medical University, Beijing, 100070, China. [3]Department of Biomedical engineering at Cornell University, Ithaca, NY 14853, USA.[4]Department of Anesthesia, Critical Care and Pain Medicine, Massachusetts General Hospital, Boston, MA 02129, USA.

[Received November 5, 2024; Revised January 13, 2025; Accepted January 14, 2025]

ABSTRACT: Studies have linked inhalation anesthesia and surgery to increased cognitive impairment, particularly in the elderly. Our previous research showed that isoflurane, but not desflurane, affected cognitive function in mice by modulating cyclophilin D (CypD), a key regulator of the mitochondrial permeability transition pore (mPTP) and mitochondrial function. Both anesthetics metabolize into trifluoroacetic acid (TFA), which is associated with cognitive deficits. However, the specific role of CypD in the TFA-induced mitochondrial dysfunction and cognitive impairments is unclear. This study aims to explore the interaction between TFA, CypD, and cognitive function in neurons and mice. TFA was administered to 2-3-month-old wild-type (WT) and CypD knockout (KO) female and male mice at 120 μg/kg and to primary cultured neurons from these mice at 10 μM. Immunofluorescence staining and Western blot analyses assessed the impact of TFA on the levels of CypD, voltage-dependent anion channel (VDAC), adenine nucleotide translocase (ANT), reactive oxygen species (ROS), and caspase-3 activation in neurons, along with cognitive function assessments in mice. The data from the present study demonstrated cognitive impairments in mice following TFA treatment. Elevated CypD and ROS levels were observed post-TFA exposure, alongside the TFA-induced caspase-3 activation in WT neurons and mice. Notably, the absence of CypD significantly mitigated these effects. The findings suggest that TFA-induced mitochondrial dysfunction, caspase-3 activation, and subsequent cognitive impairments rely on CypD expression, particularly in the hippocampus of mice. This study illuminates the molecular pathways influenced by anesthesia-related compound TFA and its impact on cognitive function.

Key words: Cognitive impairment, Trifluoroacetic Acid (TFA), Cyclophilin D (CypD)

INTRODUCTION

The Lancet Commission on Global Surgery estimates that approximately 313 million surgical procedures are performed worldwide each year, with numbers continuing to rise due to an aging population [1]. This increase highlights the pressing concern of cognitive risks associated with anesthetics and surgery, particularly in geriatric patients. Clinical studies have indicated a potential link between anesthesia, surgical procedures, and an elevated risk of developing Alzheimer's disease (AD) [2, 3]. In elderly patients, the phenomenon of perioperative neurocognitive disorder (PND) is especially significant, as it is associated with cognitive decline in the perioperative period. PND affects 12% to 40% of older adults undergoing surgery [4], posing a substantial risk as it can expedite the progression of natural cognitive decline, increasing the susceptibility to dementia and

***Correspondence should be addressed to:** Dr. Yiying Zhang, Department of Anesthesia, Critical Care and Pain Medicine, Massachusetts General Hospital and Harvard Medical School, Charlestown, MA 02129, USA. E-mail: yzhang37@mgh.harvard.edu. #The current address: Department of Anesthesia, Beijing Tiantan Hospital, Capital Medical University, Beijing, 100070, China. †The present address: Department of Biomedical engineering at Cornell University, Ithaca, NY 14853, USA.

other neurodegenerative conditions [5]. The vulnerability of geriatric patients to PND underscores the need for a better understanding of its mechanisms, which are believed to involve neuroinflammation, neuronal injury, and other physiological changes [6]. Understanding PND's mechanisms and risk factors is crucial for developing effective prevention and management strategies, which could improve outcomes and enhance the quality of life for aging populations.

Recent studies have emphasized the neurotoxic effects of certain inhalation anesthetics [7], while there are conflicting findings in the literature [8, 9]. Commonly used inhalational anesthetics belong to the class of fluorinated ethers, such as isoflurane, sevoflurane, desflurane, and others [10]. Isoflurane, a frequently utilized anesthetic, has been associated with neurotoxicity in animal studies [11]. This includes impairments in learning and memory [12, 13], mitochondrial dysfunction [9, 14], caspase activation [15, 16] and apoptosis [17, 18]. On the contrary, desflurane, another volatile anesthetic has not been linked to these adverse effects [9, 11]. Nevertheless, the underlying mechanisms that explain the differences between isoflurane and desflurane remain largely unknown.

Most halogenated volatile agents are metabolized into trifluoroacetic acid (TFA) [19]. Due to their distinct chemical structures, serum TFA levels from isoflurane are ten times higher than those from desflurane [20], with peak urinary TFA excretion after isoflurane exposure around 100 times greater than after desflurane exposure [21, 22]. TFA has been shown to be toxic. Specifically, Animal studies have shown the neurotoxic and hepatotoxic effects of TFA and its metabolites [23, 24]. TFA exposure can irritate the skin, eyes, and respiratory system [25], and prolonged or high-level exposure may result in severe tissue damage [26]. Perfluorooctanoic acid (PFOA) is an analogue of TFA, and PFOA has been shown to significantly increase levels of reactive oxygen species (ROS) and mitochondrial superoxide production, ultimately leading to apoptosis or necrosis [27]. PFOA has been shown to stimulate mitochondrial biogenesis and gene transcription in rats [28]. Despite the significant difference in TFA levels in the blood between isoflurane and desflurane exposure, the impact of TFA on cognitive function and the underlying mechanisms remains largely unknown.

In our previous research, we investigated the impact of Cyclophilin D (CypD) on mitochondrial dysfunction and neurotoxicity in the brain, leading to cognitive impairment [29, 30]. CypD, encoded by the Ppif gene, is situated in the mitochondrial matrix and is essential for mitochondrial permeability transition pore (mPTP) and mitochondrial function [31, 32]. CypD binds to adenine nucleotide translocase (ANT), another component of the mPTP [33]. Increased CypD expression is observed in the brain tissue of AD transgenic mice, contributing to AD neuropathogenesis [34, 35]. Knockout of CypD enhances mitochondrial function, reduces the mPTP formation threshold, and enhances cognitive function in elderly AD transgenic mice [34-37]. CypD may also be involved in developmental anesthesia neurotoxicity, necessitating further investigation into brain neurotoxicity [29, 30].

Building on these findings, we hypothesize that TFA may elevate reactive oxygen species (ROS) within mitochondria by upregulating CypD expression, leading to mitochondrial dysfunction. This process could, in turn, lead to caspase-3 activation, triggering apoptosis in hippocampal neurons and resulting in cognitive impairments in mice. Our objective is to elucidate the impact of TFA on neuronal health and cognitive function, aiming to advance our understanding of its effects on the nervous system and cognitive function.

MATERIALS AND METHODS

Mice TFA treatment

The animal study protocol was approved by the Massachusetts General Hospital's Standing Committee on Animals in Boston, MA, which oversees research and teaching involving animals. Compliance with the National Institutes of Health (Bethesda, MD) guidelines was ensured throughout our animal studies. We employed all possible measures to minimize the mouse population utilized in our experiments.

The study utilized wild-type (WT) C57BL/6J mice (Strain #: 000664, RRID: IMSR_JAX:000664, Common Name: B6; also known as B6J or B6/J) and CypD homozygous null (CypD KO) mice (Strain #: 022308, RRID: IMSR_JAX:022308, Common Name: CypD-KO). Specifically, the CypD KO mice were B6;129-Ppiftm1Maf/J (Ppif−/−) mice. All mice were purchased from the Jackson Laboratory (Bar Harbor, ME). Our colony bred these mice for the study. The mice were maintained in an environmentally controlled facility with regulated temperature (20 – 22°C) and humidity, under a reversed 12-hour light and dark cycle. They had unrestricted access to food and water at all times. We wrote the manuscript according to Animal Research: Reporting of In Vivo Experiments (ARRIVE).

Considering the sexually dimorphic impacts of TFA-induced neurotoxicity, we ensured a balanced ratio of female and male mice in both the TFA exposure and control groups. To uphold impartiality, mice of the same genotypes were randomly allocated to either the TFA treatment group or the untreated control group, with due regard to their gender.

Two to three months old WT mice and age-matched CypD homozygous null mice underwent the treatment with TFA or saline, where each mouse in the TFA group received a dose of 120 μg/kg TFA (CAS # 76-05-1, Sigma, St. Louis, MO) dissolved in saline, intended for behavioral alteration assessment. Conversely, the control group mice were administered an equivalent volume of saline alone. Previous clinical studies showed that plasma TFA concentrations after 1.3 MAC isoflurane treatment for 8 hours reached 15 μM on postoperative day 1, and even higher levels on postoperative days 2-4 in patients [38]. Immunohistochemical staining of hepatocytes using affinity-purified rabbit anti-TFA IgG revealed intense TFA-labeled protein staining in hepatocytes from rats exposed to isoflurane, but not in those exposed to desflurane [39]. In another study, measurements of TFA in the plasma of seven patients who had received isoflurane as an anesthetic showed concentrations ranging from 18 mmol/L (2 mg/L) in one patient, up to 100 mmol/L in a second, and 194 mmol/L in a third patient [40]. Based on the above evidence, we chose a compromise dose of 15 μM TFA for isoflurane treatment in mice. The dose calculation is as follows:

First, we calculate the molarity of the stock solution (Initial concentration: 100 g/L, Molecular weight: 114.02 g/mol):

$$\text{Concentration} = \frac{100\ \text{g/L}}{114.02\ \text{g/mol}} = 0.877\ \text{mol/L}$$

This means that 1 μL of the stock solution contains 0.877 μmol of TFA.

Next, we consider the total blood volume of a mouse, which is approximately 0.75 mL per 10 gram of body weight (BW). For a 25-gram body weight mouse, the blood volume is:

$$\text{Blood volume} = \frac{0.75\ \text{mL}}{10\ \text{g}} \times 25\ \text{g} = 1.875\ \text{mL}$$

To achieve a serum concentration of 15 μM TFA, the required dose of TFA is:

$$\text{Dose} = \frac{1.875\ \text{mL} \times 15\ \mu\text{mol/L}}{0.877\ \mu\text{mol}/\mu\text{L}} = 0.032\ \mu\text{L}$$

Therefore, the dose of TFA for each adult mouse is 0.032 μL to achieve a 15 μM TFA serum concentration.

Based on the body weight of the mice, the required dose of TFA solution is approximately 120 μg/kg.

Ten mice comprised each experimental group, saline and TFA administration was executed via tail vein infusion, a method consistent with the method of previous studies [41, 42]. It is crucial to note that all animal experimentation procedures were conducted in a blinded fashion to mitigate potential bias.

Morris Water Maze (MWM) studies

The MWM test utilized a circular steel pool, measuring 150 cm in diameter and 60 cm in height, filled with water reaching 1 cm above a submerged platform of 10 cm diameter. The pool was enclosed by a black curtain and situated in a separate, visually distinct room adorned with four cues on the peripheral walls. The water's temperature was maintained at 20 °C and rendered opaque through the addition of titanium dioxide.

Following TFA administration, a 24-hour recovery period was granted to the mice. Beginning on the third day post-treatment, all mice underwent MWM training, consisting of four trials daily for a week. During each trial, mice were introduced into the pool to locate a hidden platform. The starting position varied among the pool's four quadrants. Once the platform was discovered, mice remained on it for 30 seconds. The duration taken by each mouse to find the platform was recorded as the 'escape latency'. In instances where a mouse failed to locate the platform within 90 seconds, the mouse was gently guided to the platform and also allowed a 30 second stay. The entire process was surveilled by a video tracking system, with motion data subsequently analyzed using specialized MWM motion-detection software to evaluate performance.

Upon the completion of the standard training regimen, the platform was removed from the pool, and mice were introduced into a randomly selected quadrant for a probe trial. Each mouse was permitted to swim freely for 90 seconds, during which the frequency of crossings over the former platform location (designated as 'platform crossing times') was documented. The metrics of 'escape latency' and 'platform crossing times' were both registered as indicators of cognitive function.

To preserve the mice's core temperatures, active heating methods akin to those detailed in the reference were employed [43, 44]. This entailed drying each mouse with a heat lamp following every trial before the mouse was returned to the cage. It is important to note that the mice participating in the MWM experiments were exclusively utilized for cognitive assessments.

Barnes Maze (BM) studies

The Barnes Maze (BM) test was conducted following methods described in previous studies [41, 45-49], with some modifications. The maze consisted of a circular open platform approximately 90 cm in diameter, placed in a quiet area. It featured 20 equally spaced holes, one of which connected to a small dark recessed chamber known as the escape box. The maze was surrounded by a dark curtain with four simple colored-paper shapes (square, circle, triangle, and star) serving as spatial markers

(Stoelting, Wood Dale, IL). A video camera positioned directly above the platform captured the entire maze and was connected to the Any-Maze animal tracking system software (Stoelting Co., Wood Dale, IL), as described in previous studies [47, 50, 51].

The BM test in this study included two phases: BM training (conducted on days 10–14 after treatment of TFA) and BM testing (conducted on day 11 after treatment of TFA). Barnes Maze Training: The training phase consisted of two trials per day, each lasting 3 minutes, with a 15-minute rest period between trials. During each trial, the mouse was placed under a bucket at the center of the platform for 10 seconds before being released to locate the escape box under the aversive stimulation of bright light (200 W) and noise (85 dB). Once the mouse reached the escape box, it was allowed to remain inside for 1 minute before being returned to its home cage for the rest of period. If the mouse failed to locate the escape box within 3 minutes, the mouse was gently guided to the escape box, and the buzzer was turned off upon entry. The maze was cleaned with a 75% alcohol solution between trials to eliminate olfactory cues. On day 14 after the treatment with TFA or saline, mice underwent BM testing after being habituated to the maze. During the training phase, we measured and recorded the latency to locate and enter the escape box as well as the escape speed. In the testing phase, we recorded the latency to locate and enter the escape box, total distance traveled, the number of incorrect holes searched, and the time spent in the target zone [46-49]. A decrease in escape speed was considered indicative of impaired locomotor activity. Based on prior studies [50, 52], we used the time spent in the target quadrant rather than target preference as a measure in the current study.

Harvest of mice brain tissues

For the Western blotting assays and ROS evaluations, we harvested hippocampal tissues of mice following the protocols established in our prior research [30]. After the MWM and BM test, mice were humanely euthanized via decapitation. The brain tissues were swiftly extracted, and the hippocampi were meticulously dissected and immediately flash-frozen in liquid nitrogen in anticipation of future analyses for Western blot and ROS quantification.

Cultivation and Treatment of Neurons

In the cultivation and treatment of neurons, we adhered to techniques outlined in our previous research [29]. Pregnant mice at gestational day 15 were euthanized using carbon dioxide, followed by a cesarean section to retrieve embryos. Embryos were decapitated in a phosphate-buffered saline (PBS) solution within a sterile dish. Subsequently, cortices were carefully isolated, meninges were discarded, and neuronal tissues were transferred to a fresh PBS-filled dish. Neuronal cells were released through enzymatic digestion with trypsin and mechanical trituration. Following dissociation, neurons were resuspended in serum-free B27/neurobasal media and plated onto 6-well plates at a density ensuring 50% confluence.

Approximately 7 to 10 days post-isolation, these cultured neurons underwent a 6-hour incubation with either a standard enrichment medium or the same medium supplemented with an additional 10 μM TFA. This treatment facilitated the assessment of ROS production, caspase-3 activation, and also served as preparation for immunofluorescence staining experiments.

Western blot analysis

Hippocampal tissue samples were gently homogenized under cold conditions in an immunoprecipitation buffer composed of 10 mM Tris-HCl (pH 7.4), 150 mM sodium chloride, 2 mM ethylenediaminetetraacetic acid (EDTA), and 0.5% Nonidet P-40, complemented with protease inhibitors (1 μg/ml aprotinin, 1 μg/ml leupeptin, and 1 μg/ml pepstatin A). The lysed material was then gathered, centrifuged at 13,000 revolutions per minute for 15 minutes, and the total protein concentration was determined utilizing a bicinchoninic acid (BCA) protein assay kit procured from Pierce (Iselin, NJ).

Thereafter, both hippocampal tissues and cultured neurons underwent Western blot analysis following the methodologies detailed in our preceding study [9, 14]. Immunoblotting was conducted utilizing the following primary antibodies: anti-CypD at a 1:1000 dilution (ab110324, Abcam, Cambridge, MA, USA); anti-VDAC at a 1:1000 dilution (ab154856, Abcam); anti-ANT at a 1:1000 dilution (ab180715, Abcam); and anti-β-Actin at a 1:10,000 dilution (Sigma, St. Louis, MO, USA). A caspase-3 antibody (1:1000 dilution; Cell Signaling Technology) was employed to identify both the intact form of caspase-3 (approximately 35–40 kDa) and the cleaved fragments (around 17–20 kDa), indicative of proteolytic activation at the aspartic acid residue.

The analysis of Western blot data was conducted in a dual-step process. Initially, variations in protein loading were equalized by normalizing the target protein levels against the internal control, beta-actin. Subsequently, alterations in protein expression across different experimental groups were depicted as a percentage of the protein levels observed in the respective control conditions. Each individual band symbolized an independent experimental replicate. To obtain the final

results, data from six such independent experiments were pooled and averaged.

In brief, the densitometric quantification of the bands was carried out using the ImageJ software (version NIH Image 1.62, developed by the National Institutes of Health, Bethesda, MD). This methodology adhered closely to the protocols described in comparable prior studies, ensuring consistent and standardized data processing [14].

Measurement of ROS

Measurement of reactive oxygen species (ROS), both in vitro and in vivo, was performed according to the methodologies detailed in our previous studies [9,13]. Concisely, primary neuronal cultures were seeded into a transparent 96-well cell culture plate and incubated overnight. Next, a solution of 2',7'-dichlorodi-hydrofluorescein diacetate (DCFH-DA) was administered to the cells in culture media. Post incubation, cells were treated with 10 μM TFA for a duration of 6 hours. Thereafter, cellular lysis was induced by introducing 100 μL of lysis buffer, followed by thorough mixing and a 5-minute incubation period at ambient temperature. A volume of 150 μL from each lysate was then aliquoted into designated wells of a new 96-well plate prepared for fluorescence quantification. Regarding in vivo ROS assessments, brain tissues were processed by homogenization in ice-cold 1% Triton X-100 buffered with PBS, complemented with protease inhibitors as previously mentioned. The lysates underwent centrifugation at 10,000 rpm for 5 minutes, and protein concentrations were determined using a BCA protein assay kit (Pierce, Iselin, NJ). Triplicate 50 μL aliquots of each sample were dispensed into a black 96-well plate, combined with 50 μL of the provided catalyst solution, and incubated for 5 minutes at room temperature. Following this, 100 μL of DCFH solution from the kit was added to each well, and the plates were incubated in the dark at room temperature for an additional 20 minutes. Ultimately, fluorescence intensity was measured using a fluorometric plate reader, with excitation and emission wavelengths set at 480 nm and 530 nm, respectively.

Immunofluorescence Staining

To evaluate TFA's effect on CypD levels in the mouse hippocampus, we performed immunofluorescence as follows: extracted brains were fixed in 4% paraformaldehyde (PFA) overnight at room temperature. After washing with PBS, tissues were dehydrated in a graded ethanol series (70%, 80%, 95%, and 100%) for 1 hour each and then cleared in xylene for 2 hours. Tissues were infiltrated with paraffin wax at 60 °C for 2–3 hours before being embedded in paraffin blocks and allowed to cool. Paraffin blocks were sectioned at 5 μm thickness using a microtome. Coronal sections of the hippocampus (approximately −4.8 mm behind bregma) were mounted on glass slides, dried overnight at 37 °C, and stored at room temperature until use. Sections were fixed again in 4% PFA for 20 minutes at room temperature, then permeabilized with 0.1% Triton X-100 for 30 minutes. After blocking with 10% goat serum in PBS for 1 hour, sections were incubated overnight at 4 °C with the primary antibody (anti-CypD, 1:200, ab110324, Abcam). Following PBS washes, sections were incubated with FITC- or TRITC-conjugated secondary antibodies for 2 hours at room temperature. Nuclei were counterstained with DAPI (1:1000, Abcam) for 5 minutes. Finally, sections were washed, mounted in antifade medium, and visualized with a laser confocal microscope (TSC SP2, Leica, Mannheim, Germany).

Statistics

The statistical methods and analyses used in the study are appropriately rigorous and transparently reported. The assumptions of these statistical tests were met by the data. The biochemical data and the MWM escape latency outcomes were expressed as mean ± standard deviation (SD) or mean ± standard error of mean (SEM). Given that the frequency of platform crossings in the MWM did not conform to a normal distribution, these results were depicted as the median alongside interquartile ranges. Latency outcome values for the BM were analyzed in the same manner as those for the MWM.

Sample sizes were configured as follows: 10 animals per group for behavioral experiments; 6 samples per group for Western blot analyses of CypD, ANT, VDAC, ROS, and fluorescence staining procedures; and another 6 per group for Western blot assessments focusing on caspase-3 measurement. Statistical evaluations comprised one-way or two-way ANOVA, Student's t-tests with Bonferroni post-correction, and Mann–Whitney U tests, with statistical significance established at $P < 0.05$.

To determine the interactions between time and group variables, a two-way ANOVA with repeated measures was used to compare the learning trajectories, as inferred from escape latencies and speed, between the control and TFA-treated mice in both the MWM and BM tests. Separate Student's t-tests, with Bonferroni corrections, were employed to evaluate daily differences in escape latency and movement speed between the control and TFA groups during training days. The Mann-Whitney U test was used to identify the differences in platform crossing frequencies in the MWM testing and the number of wrong holes searched in the BM testing between the two treatment conditions. Additionally, a Student's t-test

with Bonferroni adjustment was applied to assess discrepancies in escape latency, percent time spent in the target zone, and total movement distances in the BM testing. Notably, there were no missing data points concerning the MWM and BM parameters—escape latency, platform crossing instances, and swimming velocity—throughout the statistical assessment. All statistical computations were facilitated by GraphPad Prism software, version 9.0.

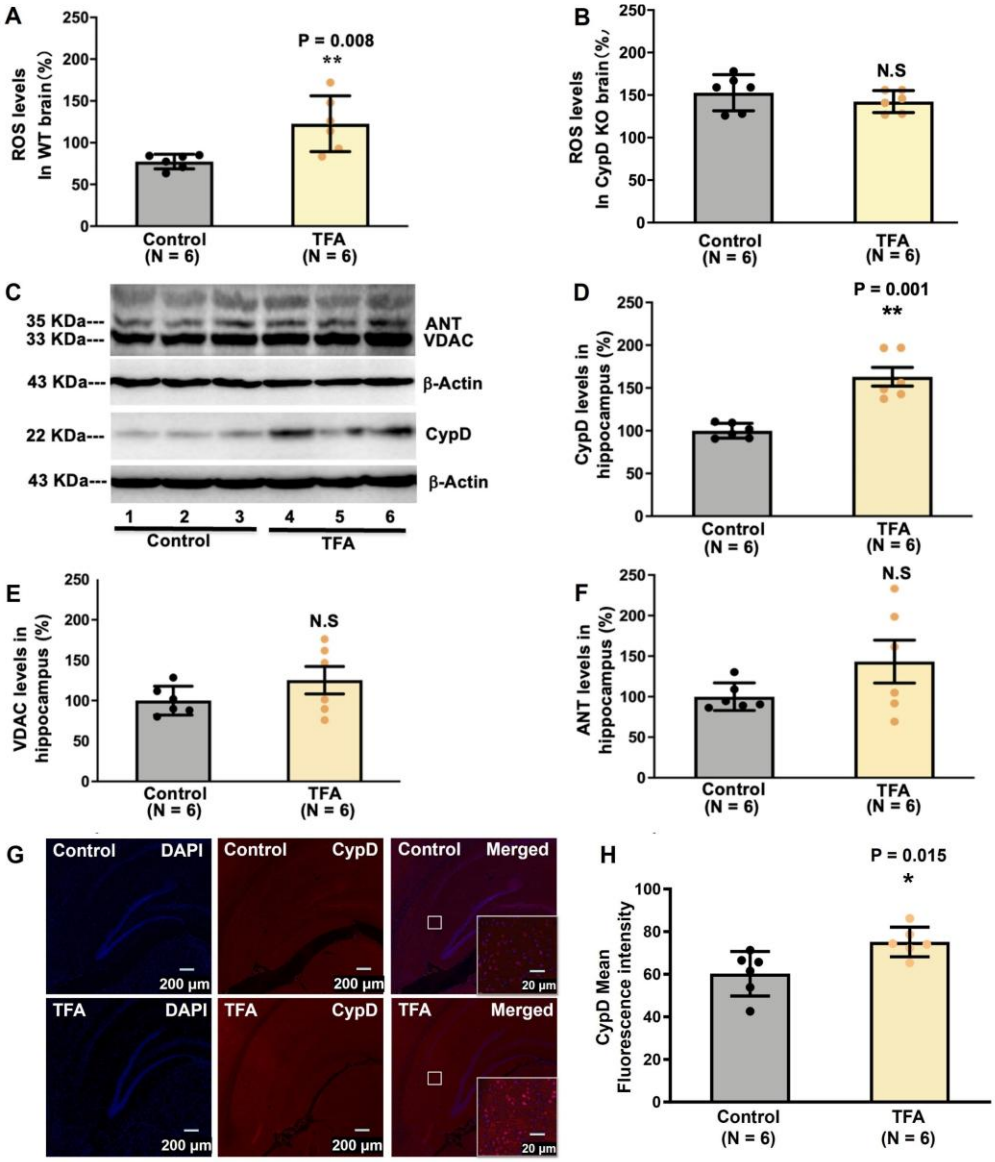

Figure 1. TFA increases ROS production and CypD protein levels in WT mice, but not in CypD KO mice. (A) TFA treatment (yellow bar) increases ROS levels as compared to the control condition (grey bar) in the hippocampus tissues of WT mice. (**P = 0.008, N = 6). **(B)** TFA treatment (yellow bar) does not significantly change the ROS levels as compared to the control condition (grey bar) in the hippocampus tissues of CypD KO mice (N = 6). **(C)** Western blot shows that TFA treatment (lanes 4–6) increases the levels of CypD, but not ANT or VDAC, the other two components of mPTP, as compared to the control condition (lanes 1–3) in the hippocampus tissues of WT mice. There is no significant difference in the amounts of β-Actin in the hippocampus tissues between the mice in the control condition group and the mice in the TFA treatment group. **(D)** Quantitation of the Western blot illustrates the increased amounts of CypD following the TFA treatment (yellow bar) compared to the control condition (grey bar, N = 6 in each group, **P = 0.001). There were no significant differences in the levels of VDAC **(E)** and ANT **(F)** in the hippocampus compared to the control condition. **(G)**. Representative images of immunofluorescent staining of CypD and DAPI in the hippocampus tissues harvested from WT mice. **(H)** Quantitation of the images illustrates the increased amounts of CypD following TFA treatment compared to the control condition in WT mice (N = 6 in each group, *P = 0.015). Trifluoroacetic acid (TFA), Cyclophilin D (CypD), reactive oxygen species (ROS), voltage-dependent anion channel (VDAC), adenosine nucleotide translocase (ANT), knock out (KO), N.S: non-significant differences.

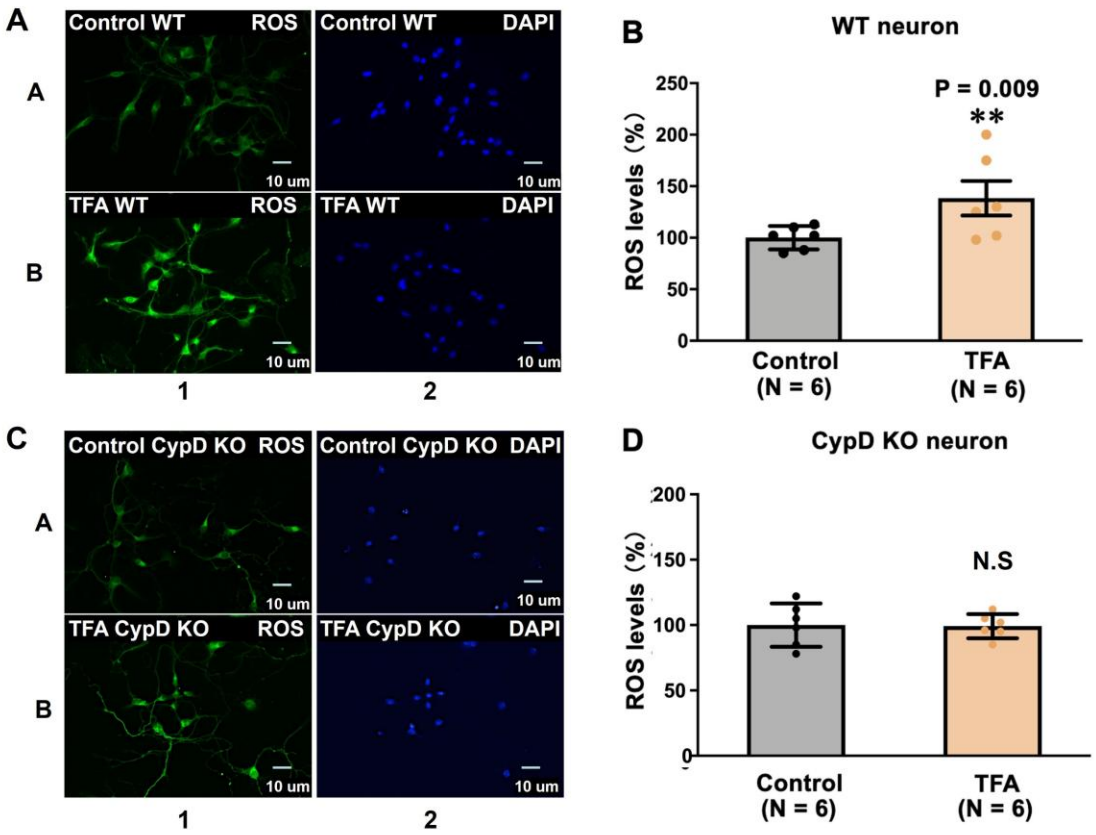

Figure 2. TFA increases ROS levels in WT mice neurons, but not in CypD KO mice neurons. (A) Representative images of immunofluorescent staining of ROS and DAPI harvested from WT neurons. Column 1 is the ROS (green) staining, column 2 is the DAPI (blue) staining. TFA treatment (row B) increases ROS levels compared to the control condition (row A) in WT neurons. **(B)** Quantitation of the image illustrates increased amounts of ROS levels following TFA treatment compared to the control condition (N = 6 in each group, **P = 0.009). **(C)** Representative images of immunofluorescent staining of ROS and DAPI harvested from CypD KO neurons. TFA treatment (row B) does not change levels of ROS compared to the control condition (row A) in CypD KO neurons. **(D)** Quantitation of the image illustrates that there is no significant difference in ROS levels between the TFA treatment and the control condition in CypD KO neurons (N = 6 in each group). Trifluoroacetic acid (TFA), Cyclophilin D (CypD), reactive oxygen species (ROS), knock out (KO), N.S: non-significant differences.

RESULTS

TFA increased ROS and CypD levels in WT mice, but not in CypD KO mice

Our initial findings suggest that treatment with TFA increased the levels of ROS in hippocampal tissues obtained from WT mice compared to the control condition (Fig. 1A, **P = 0.008, Student's t-test), while there were no significant differences in ROS levels in hippocampal tissues from CypD KO mice (Fig. 1B). We next analyzed the levels of CypD protein in the WT mice hippocampus using Western blot. Western blot analysis of CypD indicated a substantial increase in CypD levels in response to TFA treatment, distinct from ANT and VDAC, the other two components of the mPTP, as compared to the control condition (Fig. 1C). Quantitative analysis of the Western blot, based on the ratio of CypD level to β-actin level, revealed a significant rise in CypD levels within the hippocampus following TFA treatment (Fig. 1D, **P = 0.001, Student's t-test). This surge was exclusive to CypD, as it did not affect the levels of VDAC and ANT in the hippocampus (Fig. 1E, 1F). To further confirm the changes in CypD levels in the mouse hippocampus following TFA treatment. The immunofluorescence staining showed an increase in CypD fluorescence in the hippocampus of WT mice after TFA injection compared to the control condition (Fig. 1G). Quantification of the images revealed a significant increase in fluorescence intensity in the hippocampus of TFA-treated WT mice compared to the control (Fig. 1H, * P = 0.015, Student's t-test).

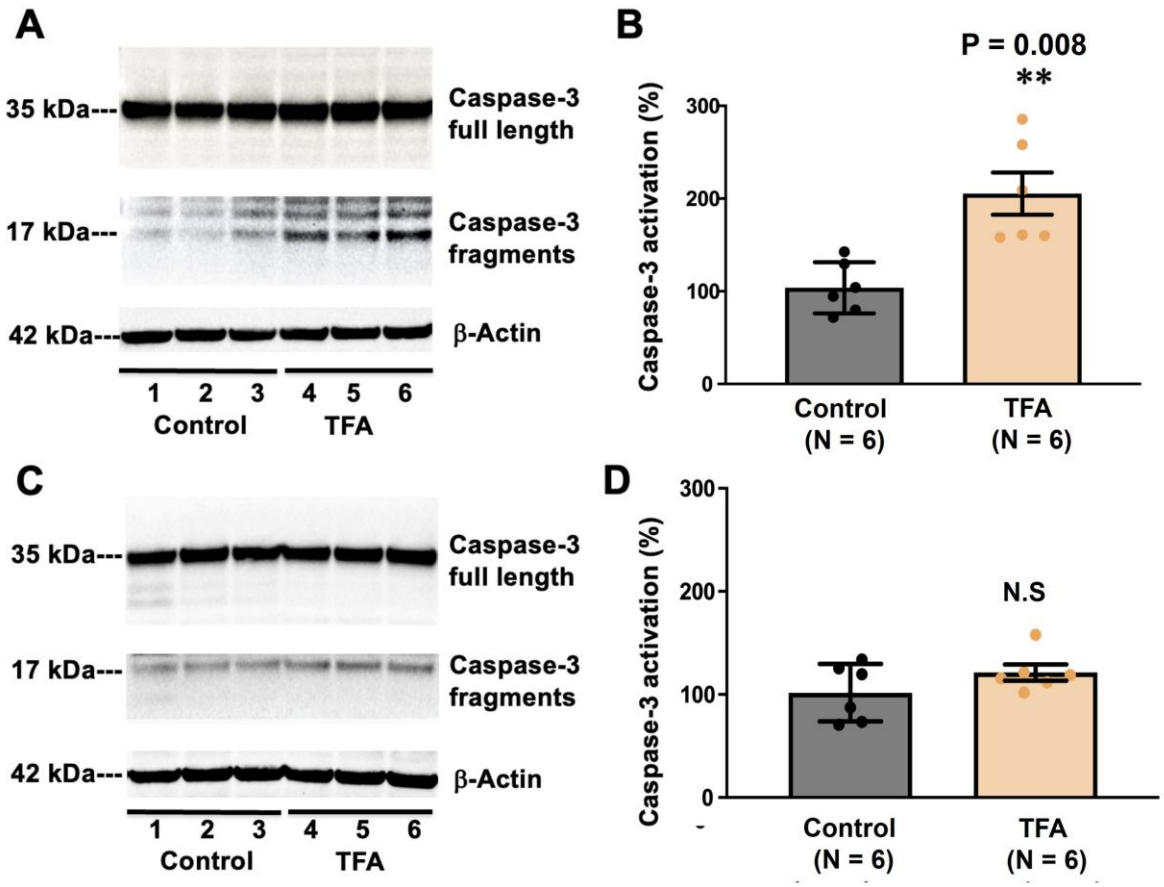

Figure 3. TFA induces caspase-3 activation in WT neurons, but not in CypD KO neurons. (A) Western blot shows that the TFA treatment (lanes 4 to 6) discernibly increases the levels of caspase-3 fragments in WT neurons compared to the control condition (lanes 1 to 3). There is no significant difference in β-actin levels between the TFA treatment and control condition. **(B)** Quantitation of the Western blot illustrates increased levels of caspase-3 activation in WT neurons following the TFA treatment compared to the control condition (N = 6 in each group, **P = 0.008). **(C)** Western blot shows that there is no significant difference of caspase-3 fragments in CypD KO neurons between TFA treatment (lanes 4 to 6) and control condition (lanes 1 to 3). **(D)** Quantitation of the Western blot shows that the TFA treatment does not affect the levels of caspase-3 activation in CypD KO neurons compared to the control condition (N = 6 in each group). Trifluoroacetic acid (TFA), Cyclophilin D (CypD), knock out (KO), N.S: non-significant differences.

The TFA treatment increased ROS levels and induced caspase-3 activation in cultured WT mice neurons, but not in CypD KO mice neurons

To investigate the role of CypD in TFA-induced effects on in vitro neurons, we used primary cultured neurons harvested from both WT and CypD KO mice in the present study. We found that immunofluorescence staining of ROS revealed a notable increase in ROS levels in the cultured neurons harvested from WT mice following the TFA treatment compared to the control condition (Fig. 2A). Quantification of the immunofluorescence staining also demonstrated a significant increase in ROS levels in WT mice neurons following the TFA treatment compared to the control condition (Fig. 2B, **P = 0.009, Student's t-test). Conversely, immunofluorescence staining of ROS in neurons harvested from CypD KO mice indicated no substantial alteration in ROS levels following the TFA treatment compared to the control condition (Fig. 2C). Quantification of the immunofluorescence staining also showed that there was no significant difference in ROS levels in CypD KO neurons between the TFA treatment and the control condition (Fig. 2D).

Immunoblotting of caspase-3 fragments illustrated that the TFA treatment induced caspase-3 activation in the primary cultured neurons harvested from WT mice, as evidenced by the comparison of the bands from TFA treatment (lanes 4 to 6) and control condition (lanes 1 to 3) (Fig. 3A). There was no significant difference in β-actin levels between these two groups. Quantification of the Western blot demonstrated a significant increase in

caspase-3 activation levels in neurons harvested from WT mice following the TFA treatment (Fig. 3B, ** P = 0.008, Student's t-test). Conversely, immunoblotting revealed no substantial distinctions in caspase-3 fragments in CypD KO neurons between the TFA treatment and control condition (Fig. 3C). Quantification of the Western blot further showed that there was no significant difference in caspase-3 activation in CypD KO neurons between the TFA treatment and control condition (Fig. 3D).

TFA-triggered cognitive impairments were dependent on CypD in WT mice, whereas CypD KO ameliorated the TFA-induced cognitive impairment in mice.

Building upon the in vitro findings that implicated a CypD-dependent role in TFA-induced increases in ROS levels and caspase-3 activation, we set out to investigate the in vivo relevance of these findings using Morris Water Maze (MWM) and Barnes Maze (BM) studies in 2-3-month-old WT and CypD KO mice. A diagram of the treatment and behavioral test schedule, including a scheme of the behavioral test and the timeline for the training and testing days, is shown in Figure 4A.

First, we assessed the baseline cognitive functions of WT and CypD KO mice using the MWM. No significant behavioral differences were observed between the WT and CypD KO mice at baseline, confirming that both groups started with comparable cognitive functions (Supplementary Fig. 3).

Then, utilizing a Two-way ANOVA with repeated measurement, we observed no statistically significant difference in time and treatment (TFA vs. control condition) on the escape latency in MWM training days for both WT and CypD KO mice (Fig. 4B, 4E). However, the Mann-Whitney test showed that the TFA treatment decreased the platform crossing times of WT mice compared to the control condition on testing day (Fig. 4C, ** P = 0.008, Mann-Whitney test). Conversely, CypD KO mice displayed no differences in platform crossing times between the TFA treatment and the control condition (Fig. 4F). Furthermore, there were no significant differences in swimming speed for both WT and CypD KO mice between the TFA treatment and the control condition on the training days (Fig. 4D, 4G). Next, we used the BM to confirm the cognitive dysfunction caused by TFA. A two-way ANOVA with repeated measures revealed a significant interaction between time and treatment (TFA vs. control condition) on escape latency during the BM training days, particularly on day 13 for WT mice (Fig. 4H, F = 4.742, ** P = 0.005). Furthermore, a Student's t-test showed that TFA treatment significantly increased the escape latency of WT mice compared to the control condition on the BM testing day (Fig. 4I, ** P = 0.001). Additionally, the Mann-Whitney U test indicated that TFA treatment increased the number of wrong holes searched by WT mice compared to the control condition on the testing day (Fig. 4K, * P = 0.034). However, there were no significant differences in the time spent in the target zone or total movement distances for WT mice between the TFA treatment and the control condition on the BM testing day (Fig. 4J, 4L). And there were no significant differences in movement speed for WT mice between the TFA treatment and the control condition on the training day (Fig. 4M).

Recent evidence indicates gender disparities in dementia, with females showing higher vulnerability to age-related cognitive decline. Therefore, we stratify the MWM dataset by gender to explore gender variations in TFA-induced cognitive deficits in wild-type and CypD KO mice.

In our results, there's no statistical significance in time and treatment (TFA injection vs. control condition) on the escape latency in MWM training days for both female and male WT mice (Supplementary Fig. 1A). While it's noteworthy that the TFA treatment in the female WT mice decreased the platform crossing times as compared to the control condition (* P = 0.034, Supplementary Fig. 1B), but didn't in the male WT mice (Supplementary Fig. 1B). In addition, there was no significant difference in swimming speed for female and male WT mice between the TFA treatment and the control condition on the testing day (Supplementary Fig. 1C). On the contrary, CypD KO mice displayed no sex difference in the escape latency (Supplementary Fig. 2A) and swimming speed (Supplementary Fig. 2C) in MWM training days, and platform crossing times on testing day between the TFA treatment and the control condition (Supplementary Fig. 2B).

Taken together, these data suggest that treatment with TFA increases ROS accumulation and CypD levels and, which may partially contribute to the observed caspase-3 activation in cultured hippocampal neurons and mouse brain tissue. This, in turn, may lead to cognitive impairments in WT mice (Fig. 5), pending further confirmatory investigation.

DISCUSSION

In the present research, we have discovered that TFA can instigate CypD-dependent mitochondrial dysfunction and caspase-3 activation, both in vivo and in vitro. These changes lead to compromised learning and memory in mice. Notably, it has been established that isoflurane, but not desflurane, induces mitochondrial dysfunction, caspase-3 activation, cytotoxicity, and impairs learning and memory in mice [9, 13, 14]. TFA, which is a metabolite of both isoflurane and desflurane, exhibits a significant disparity in serum concentration, with

isoflurane levels approximately 10 times higher than those of desflurane [20, 22, 53]. We employed TFA as a tool to elucidate the underlying mechanisms potentially responsible for the neurotoxic disparities and cognitive effects induced by desflurane and isoflurane, with particular emphasis on the role of CypD, mitochondrial function, caspase-3 activation, and cognition in mice. These data are consistent with the findings from previous studies that anesthetics may damage mitochondrial function [54]. Future studies will further test the hypothesis generated in this proof-of-concept study.

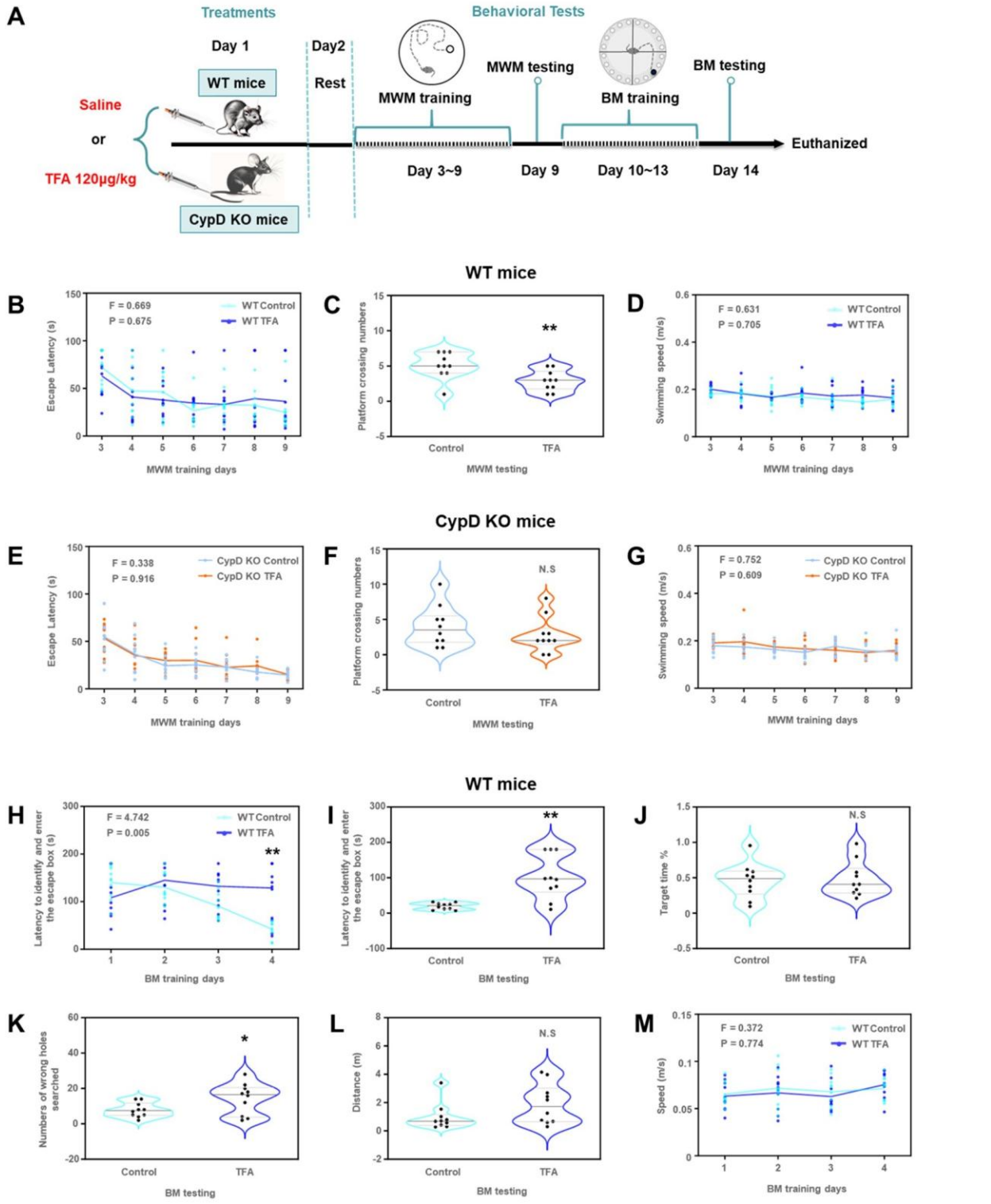

Figure 4. TFA induces a CypD-dependent cognitive impairment in mice. (A) Experimental design and timeline. **(B)** Two-way ANOVA with repeated measurement analysis shows no significant interaction between the treatment (TFA treatment and control condition) and time on escape latency (N = 10 in each group, F = 0.669, P = 0.675) in the WT mice during training days of MWM. **(C)** The Mann-Whitney test shows that the WT mice following TFA treatment have fewer platform crossing numbers than the WT mice following the control condition on the testing day of MWM (N = 10 in each group, **P = 0.008). **(D)** There are no significant differences in swimming speed between each treatment during training days in WT mice. **(E)** Two-way ANOVA with repeated measurement analysis shows no significant interaction between the treatment (TFA treatment and control condition) and time on escape latency during training days of MWM in the CypD KO mice (N = 10 in each group, F = 0.338, P = 0.916). **(F)** The Mann-Whitney test shows that there is no significant difference in platform crossing numbers on the testing day of MWM between the TFA treatment and the control condition in CypD KO mice (N = 10 in each group). **(G)** There are no significant differences in swimming speed between each treatment during training days in CypD KO mice. BM studies show increased latency to enter escape box during BM training days (**H**), and increased latency to enter escape box on BM testing day (**I**), no change of BM target time on testing day (**J**), increased number of wrong holes searched on BM testing day (**K**), and no change of distance on testing day (**L**) and speed during BM training days (**M**) compared to the control group in WT mice (N = 10 in each group). Morris water maze (MWM), Trifluoroacetic acid (TFA), Cyclophilin D (CypD), knock out (KO), N.S: non-significant differences. BM, Barnes maze.

Desflurane is preferred for its minimal metabolism, which contributes to its rapid and predictable emergence from anesthesia. Metabolically, desflurane generates fluoride ions, nonvolatile organic fluoride, and TFA through a minor hepatic oxidative process, although this metabolic pathway has little impact on the drug's clearance from the body. On the other hand, isoflurane, while also exhaled unchanged from the lungs, undergoes a slightly more extensive metabolism in comparison to desflurane [20]. This metabolism results in the production of TFA and inorganic fluoride as metabolites, although it is generally considered minor in its elimination.

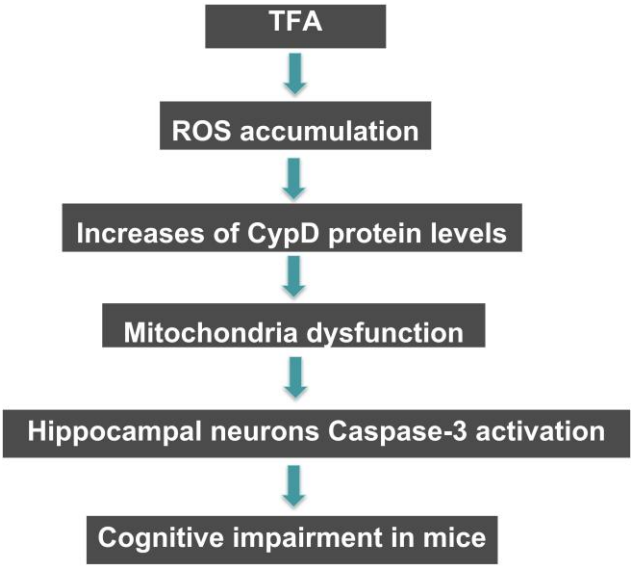

Figure 5. A proposed model illustrating the potential pathway by which CypD is linked to TFA-induced cognitive impairment in mice. TFA increases levels of ROS. The increased ROS then enhances CypD accumulation, which then causes mitochondrial dysfunction and induces caspase-3 activation in hippocampal neurons, eventually leading to cognitive impairment in mice.

Specifically, previous studies have shown notable differences in the peak serum concentration of TFA and the peak urinary excretion rate 24 hours after desflurane exposure compared to isoflurane exposure [22, 53]. Consistently, studies on TFA typically focus on its chemical properties, toxicity, and environmental impact [55, 56]. TFA is considered a hazardous chemical, and exposure to high concentrations can lead to various adverse health effects, including irritation of the respiratory tract, skin, and eyes, as well as potential systemic toxicity[57, 58].While acute exposure to high concentrations of TFA or its derivatives may cause neurological symptoms such as headaches or dizziness, there is no specific research investigating TFA's effect on cognitive impairment in animals.

In a previous study, we found that sevoflurane anesthesia increased CypD levels, potentially leading to CypD-dependent inhibition of cell proliferation, impaired migration of NPCs, and subsequent cognitive function impairment [30]. Moreover, it has been noted that isoflurane, but not desflurane, triggers mitochondrial dysfunction, caspase-3 activation, cytotoxicity, and impairs learning and memory in mice [9, 14]. Our current research reveals that TFA induces CypD-dependent mitochondrial dysfunction and caspase-3 activation in mouse neurons and hippocampus, resulting in impaired learning and memory in mice.

In addition, recent evidence suggests that gender differences exist in dementia, and females are more susceptible to developing cognitive impairment in the elderly population [59-61]. We find that female mice appeared to be sensitive to TFA treatment in comparison to their male counterparts in the testing day. To illustrate the effects of TFA with and without considering gender as a variable, we first ensured a balanced ratio of male and female mice in both the TFA treatment and control groups (Fig. 4). Mice of the same genotype were randomly assigned to either group, with gender carefully matched. We then analyzed the data separately by gender to

investigate potential differences in the TFA-induced cognitive impairments in WT and CypD KO mice. Afterward, we combined male and female data within each group to more clearly highlight the overall effects of TFA on both genders (Supplementary Fig. 1A to C and Fig. 2A to C). These findings suggested earlier findings that females are more vulnerable to developing cognitive dysfunction in the central nervous system than males. These findings reinforce earlier findings that females are more vulnerable to developing cognitive impairment than males. In future research, we will concentrate on investigating the impact of gender on cognitive function. Interestingly, male mice in the TFA group showed a trend toward shorter escape latency compared to the control group (Supplementary Fig. 1), although this was not statistically significant. Nevertheless, this observation suggests that TFA may exert distinct influences on spatial learning and memory in males and females, potentially due to sex-specific responses to TFA-induced oxidative stress. These findings are consistent with earlier research indicating that females may be more vulnerable than males to developing cognitive dysfunction. In future studies, we will focus on examining how sex-related differences influence cognitive function in vulnerable brain regions, aiming to further clarify the mechanisms underlying these effects.

This study has several limitations. First, we concentrated exclusively on the effects of trifluoroacetic acid (TFA), a primary metabolite of isoflurane and desflurane, without examining the broader spectrum of metabolites produced by other commonly used anesthetics. Future studies will broaden this focus by investigating the effects of isoflurane, desflurane, and sevoflurane, along with their respective metabolites, on mitochondrial function and cognitive outcomes. This approach will help delineate the distinct and combined contributions of various anesthetic agents and their metabolites on neurotoxicity. Second, we noted potential sex-dependent effects of TFA neurotoxicity in behavioral assays on female wild-type mice; however, no substantial biochemical differences were observed. Third, our study primarily utilized 2-3-month-old mice as a foundational system to examine TFA's neurotoxic effects. Recognizing the importance of age as a variable, future research will include aged mice to assess age-dependent responses to TFA and its influence on long-term cognitive function in aged animals. This will provide insights into how age-related mitochondrial decline and cognitive deterioration might interact with TFA exposure. Fourth, we administered TFA via tail vein infusion, but we were unable to directly measure its concentration in the mice's cerebrospinal fluid (CSF), owing to technical difficulties. To address this limitation, we used a machine learning-based prediction model (LogBB_Pred) to estimate blood-brain barrier (BBB) permeability [62]. According to this model, TFA has a logBB value of -0.18, indicating BBB permeability, comparable to ethanol (logBB = -0.18), which is known to be able to cross the BBB (Supplementary Fig. 4). Future studies should aim to develop technology to measure TFA levels in the CSF to assess sex-specific vulnerabilities in male and female mice and explore any associations with cognitive performance. Finally, our findings suggest that TFA triggers CypD-dependent cognitive dysfunction, implying that targeting CypD to mitigate TFA's harmful effects could be a viable therapeutic strategy for reducing anesthesia-related neurotoxicity. We aim to identify potential interventions that could counteract TFA's adverse impact on mitochondrial and cognitive health, ultimately working toward translating these findings into improved clinical practices and outcomes for patients undergoing anesthesia and surgery, especially within vulnerable populations such as the elderly.

Conclusions

In this proof-of-concept and hypothesis-generating research, we demonstrated that TFA induces CypD-dependent mitochondrial dysfunction, caspase-3 activation, and cognitive impairment in both mice and neuronal models. The findings suggest that TFA may induce neurotoxicity and cognitive impairment by increasing CypD levels in hippocampal neurons in mice. These results provide insights into the mechanistic exploration of neurotoxicity in the brain (refer to Fig. 5). Consequently, mitigating the detrimental effects of TFA resulting from certain high-productivity inhalational anesthetics could serve as a potential effective prevention strategy for anesthesia-induced neurotoxicity. Additionally, targeting CypD therapeutically to counteract its excessive activity could present a novel treatment approach for targeted interventions in anesthesia-induced neurotoxicity and neurobehavioral impairments, pending further investigation.

Acknowledgments

We gratefully acknowledge the funding support for this study provided by the National Institutes of Health through R21 AG065606 (awarded to Yiying Zhang), R01 HD086977, and RF1070761 and 1R01AG070257-01 (awarded to Zhongcong Xie). We would like to thank Shuyuan Gan from Massachusetts General Hospital for her valuable comments and insightful discussions. The experiments were conducted by the first and second authors at Geriatric Anesthesia Research Unit, Department of Anesthesia, Critical Care and Pain Medicine, Massachusetts General Hospital and Harvard

Medical School, Charlestown, MA 02129, USA. Presently, Dr. Yun Li is affiliated with Beijing Tiantan Hospital, while Dr. Yichi Xu is associated with Cornell University. Dr. Yun Li was partly supported by the National Natural Science Foundation of China (grant number 82101260) only during the phase of writing and submitting the manuscript, following Dr. Li's return to China after completing the experiments in Massachusetts General Hospital and Harvard Medical School.

Author contributions

Yun Li: Conceptualization, methodology, formal analysis, writing—original draft, writing—review and editing. Yichi Xu: Methodology, Data curation. Yuanlin Dong: Software, validation, visualization. Christa J. Nehs: Resources, project administration, supervision. Zhongcong Xie: conceptualization, funding acquisition, resources supplies, data curation, and revision of manuscript. Yiying Zhang: conceptualization, funding acquisition, supervision, methodology, formal analysis of data, validation, writing—review and editing of manuscript.

Conflicts of Interest

The authors declare that they have no financial disclosure related to the present study. Dr. Zhongcong Xie provided consulting services to Baxter, NanoMosaic, Shanghai Fourth, Ninth, and Tenth Hospitals, the Shanghai Mental Health Center affiliated with Shanghai Jiao Tong University School of Medicine, and the journal Anesthesiology and Perioperative Science within the past 36 months, but is not currently engaged in any of these roles.

Data Availability

The research data was provided in file Original data 1.

Institutional Review Board Statement

The protocol of the animal study was approved by the Massachusetts General Hospital Standing Committee on Animals (Boston) on the use of Animals in Research and Teaching. We performed animal studies according to the regulations of the National Institutes of Health (Bethesda, MD).

Supplementary Materials

The Supplementary data can be found online at: www.aginganddisease.org/EN/10.14336/AD.2024.1430.

References

[1] Meara JG, Leather AJ, Hagander L, Alkire BC, Alonso N, Ameh EA, Bickler SW, Conteh L, Dare AJ, Davies J, Mérisier ED, El-Halabi S, Farmer PE, et al. (2015). Global Surgery 2030: evidence and solutions for achieving health, welfare, and economic development. Lancet, 386(9993):569-624.

[2] Jiang J, Dong Y, Huang W and Bao M (2017). General anesthesia exposure and risk of dementia: a meta-analysis of epidemiological studies. Oncotarget, 8(35):59628-37.

[3] Kim CT, Myung W, Lewis M, Lee H, Kim SE, Lee K, Lee C, Choi J, Kim H, Carroll BJ and Kim DK (2018). Exposure to General Anesthesia and Risk of Dementia: A Nationwide Population-Based Cohort Study. J Alzheimers Dis, 63(1):395-405.

[4] Zhang L, Qiu Y, Zhang ZF, Zhao YF and Ding YM (2024). Current perspectives on postoperative cognitive dysfunction in geriatric patients: insights from clinical practice. Front Med (Lausanne), 11:1466681.

[5] Wang YW, Wang L, Yuan SJ, Zhang Y, Zhang X and Zhou LT (2022). Postoperative Cognitive Dysfunction and Alzheimer's Disease: A Transcriptome-Based Comparison of Animal Models. Front Aging Neurosci, 14:900350.

[6] Li Z, Zhu Y, Kang Y, Qin S and Chai J (2022). Neuroinflammation as the Underlying Mechanism of Postoperative Cognitive Dysfunction and Therapeutic Strategies. Front Cell Neurosci, 16:843069.

[7] Vutskits L and Xie Z (2016). Lasting impact of general anaesthesia on the brain: mechanisms and relevance. Nat Rev Neurosci, 17(11):705-17.

[8] Schallner N, Ulbrich F, Engelstaedter H, Biermann J, Auwaerter V, Loop T and Goebel U (2014). Isoflurane but Not Sevoflurane or Desflurane Aggravates Injury to Neurons In Vitro and In Vivo via p75NTR-NF-κB Activation. Anesth Analg, 119(6):1429-41.

[9] Zhang Y, Xu Z, Wang H, Dong Y, Shi HN, Culley DJ, Crosby G, Marcantonio ER, Tanzi RE and Xie Z (2012). Anesthetics isoflurane and desflurane differently affect mitochondrial function, learning, and memory. Ann Neurol, 71(5):687-98.

[10] Terrell Ross C and Warner David S (2008). The Invention and Development of Enflurane, Isoflurane, Sevoflurane, and Desflurane. Anesthesiology, 108(3):531-3.

[11] Zhang B, Tian M, Zhen Y, Yue Y, Sherman J, Zheng H, Li S, Tanzi RE, Marcantonio ER and Xie Z (2012). The effects of isoflurane and desflurane on cognitive function in humans. Anesth Analg, 114(2):410-5.

[12] Uchimoto K, Miyazaki T, Kamiya Y, Mihara T, Koyama Y, Taguri M, Inagawa G, Takahashi T and Goto T (2014). Isoflurane impairs learning and hippocampal long-term potentiation via the saturation of synaptic plasticity. Anesthesiology, 121(2):302-10.

[13] Zhang Y, Dong Y, Wu X, Lu Y, Xu Z, Knapp A, Yue Y, Xu T and Xie Z (2010). The mitochondrial pathway

of anesthetic isoflurane-induced apoptosis. J Biol Chem, 285(6):4025-37.

[14] Zhang Y, Dong Y, Xu Z and Xie Z (2012). Propofol and magnesium attenuate isoflurane-induced caspase-3 activation via inhibiting mitochondrial permeability transition pore. Med Gas Res, 2(1):20.

[15] Xie Z, Culley DJ, Dong Y, Zhang G, Zhang B, Moir RD, Frosch MP, Crosby G and Tanzi RE (2008). The common inhalation anesthetic isoflurane induces caspase activation and increases amyloid beta-protein level in vivo. Ann Neurol, 64(6):618-27.

[16] Zhang G, Dong Y, Zhang B, Ichinose F, Wu X, Culley DJ, Crosby G, Tanzi RE and Xie Z (2008). Isoflurane-induced caspase-3 activation is dependent on cytosolic calcium and can be attenuated by memantine. J Neurosci, 28(17):4551-60.

[17] Xie Z, Dong Y, Maeda U, Moir RD, Xia W, Culley DJ, Crosby G and Tanzi RE (2007). The inhalation anesthetic isoflurane induces a vicious cycle of apoptosis and amyloid beta-protein accumulation. J Neurosci, 27(6):1247-54.

[18] Xie Z, Dong Y, Maeda U, Moir R, Inouye SK, Culley DJ, Crosby G and Tanzi RE (2006). Isoflurane-induced apoptosis: a potential pathogenic link between delirium and dementia. J Gerontol A Biol Sci Med Sci, 61(12):1300-6.

[19] Safari S, Motavaf M, Seyed Siamdoust SA and Alavian SM (2014). Hepatotoxicity of halogenated inhalational anesthetics. Iran Red Crescent Med J, 16(9):e20153.

[20] Koblin DD (1992). Characteristics and implications of desflurane metabolism and toxicity. Anesth Analg, 75(4 Suppl):S10-6.

[21] Mazze RI, Cousins MJ and Barr GA (1974). Renal effects and metabolism of isoflurane in man. Anesthesiology, 40(6):536-42.

[22] Sutton TS, Koblin DD, Gruenke LD, Weiskopf RB, Rampil IJ, Waskell L and Eger EI (1991). Fluoride metabolites after prolonged exposure of volunteers and patients to desflurane. Anesth Analg, 73(2):180-5.

[23] Ma TG, Ling YH, McClure GD and Tseng MT (1990). Effects of trifluoroacetic acid, a halothane metabolite, on C6 glioma cells. J Toxicol Environ Health, 31(2):147-58.

[24] Gut J, Christen U, Frey N, Koch V and Stoffler D (1995). Molecular mimicry in halothane hepatitis: biochemical and structural characterization of lipoylated autoantigens. Toxicology, 97(1-3):199-224.

[25] National Center for Biotechnology Information (2025). PubChem Compound Summary for CID 12135446, Trifluoroacetic acid ammonium salt. URL: *https://pubchem.ncbi.nlm.nih.gov/compound/Trifluoroacetic-acid-ammonium-salt.*

[26] Rochlin DH, Rajasingh CM, Karanas YL and Davis DJ (2018). Full-Thickness Chemical Burn From Trifluoroacetic Acid: A Case Report and Review of the Literature. Ann Plast Surg, 81(5):528-30.

[27] Choi EM, Suh KS, Rhee SY, Oh S, Woo JT, Kim SW, Kim YS, Pak YK and Chon S (2017). Perfluorooctanoic acid induces mitochondrial dysfunction in MC3T3-E1 osteoblast cells. J Environ Sci Health A Tox Hazard Subst Environ Eng, 52(3):281-9.

[28] Walters MW, Bjork JA and Wallace KB (2009). Perfluorooctanoic acid stimulated mitochondrial biogenesis and gene transcription in rats. Toxicology, 264(1-2):10-5.

[29] Zhang Y, Lu P, Liang F, Liufu N, Dong Y, Zheng JC and Xie Z (2019). Cyclophilin D Contributes to Anesthesia Neurotoxicity in the Developing Brain. Front Cell Dev Biol, 7:396.

[30] Lu P, Liang F, Dong Y, Xie Z and Zhang Y (2023). Sevoflurane Induces a Cyclophilin D-Dependent Decrease of Neural Progenitor Cells Migration. Int J Mol Sci, 24(7):6746.

[31] Basso E, Fante L, Fowlkes J, Petronilli V, Forte MA and Bernardi P (2005). Properties of the permeability transition pore in mitochondria devoid of Cyclophilin D. J Biol Chem, 280(19):18558-61.

[32] Baines CP, Kaiser RA, Purcell NH, Blair NS, Osinska H, Hambleton MA, Brunskill EW, Sayen MR, Gottlieb RA, Dorn GW, Robbins J and Molkentin JD (2005). Loss of cyclophilin D reveals a critical role for mitochondrial permeability transition in cell death. Nature, 434(7033):658-62.

[33] Duarte FV, Gomes AP, Teodoro JS, Varela AT, Moreno AJ, Rolo AP and Palmeira CM (2013). Dibenzofuran-induced mitochondrial dysfunction: Interaction with ANT carrier. Toxicol In Vitro, 27(8):2160-8.

[34] Du H, Guo L, Fang F, Chen D, Sosunov AA, McKhann GM, Yan Y, Wang C, Zhang H, Molkentin JD, Gunn-Moore FJ, Vonsattel JP, Arancio O, et al. (2008). Cyclophilin D deficiency attenuates mitochondrial and neuronal perturbation and ameliorates learning and memory in Alzheimer's disease. Nature medicine, 14(10):1097-105.

[35] Du H, Guo L, Zhang W, Rydzewska M and Yan S (2011). Cyclophilin D deficiency improves mitochondrial function and learning/memory in aging Alzheimer disease mouse model. Neurobiol Aging, 32(3):398-406.

[36] Du H, Guo L, Wu X, Sosunov AA, McKhann GM, Chen JX and Yan SS (2014). Cyclophilin D deficiency rescues Aβ-impaired PKA/CREB signaling and alleviates synaptic degeneration. Biochim Biophys Acta, 1842(12 Pt A):2517-27.

[37] Sun J and Jacobs KM (2016). Knockout of Cyclophilin-D Provides Partial Amelioration of Intrinsic and Synaptic Properties Altered by Mild Traumatic Brain Injury. Front Syst Neurosci, 10:63.

[38] Kharasch ED, Hankins DC and Cox K (1999). Clinical isoflurane metabolism by cytochrome P450 2E1. Anesthesiology, 90(3):766-71.

[39] Njoku D, Laster MJ, Gong DH, Eger EI, 2nd, Reed GF and Martin JL (1997). Biotransformation of halothane, enflurane, isoflurane, and desflurane to trifluoroacetylated liver proteins: association between protein acylation and hepatic injury. Anesth Analg, 84(1):173-8.

[40] Morio M, Fujii K, Takiyama R, Chikasue F, Kikuchi H and Ribarić L (1980). Quantitative analysis of trifluoroacetate in the urine and blood by isotachophoresis. Anesthesiology, 53(1):56-9.

[41] Yang S, Gu C, Mandeville ET, Dong Y, Esposito E, Zhang Y, Yang G, Shen Y, Fu X, Lo EH and Xie Z (2017). Anesthesia and Surgery Impair Blood-Brain Barrier and Cognitive Function in Mice. Front Immunol, 8:902.

[42] Wu M, Zhong C, Deng Y, Zhang Q, Zhang X and Zhao X (2020). Resveratrol loaded glycyrrhizic acid-conjugated human serum albumin nanoparticles for tail vein injection II: pharmacokinetics, tissue distribution and bioavailability. Drug Deliv, 27(1):81-90.

[43] Tao G, Zhang J, Zhang L, Dong Y, Yu B, Crosby G, Culley DJ, Zhang Y and Xie Z (2014). Sevoflurane induces tau phosphorylation and glycogen synthase kinase 3beta activation in young mice. Anesthesiology, 121(3):510-27.

[44] Song S, Zhao W, Ji Y, Huang Q, Li Y, Chen S, Yang J and Jin X (2023). SHANK2 protein contributes to sevoflurane-induced developmental neurotoxicity and cognitive dysfunction in C57BL/6 male mice. Anesthesiology and Perioperative Science, 1(1):2.

[45] Liufu N, Liu L, Shen S, Jiang Z, Dong Y, Wang Y, Culley D, Crosby G, Cao M, Shen Y, Marcantonio E, Xie Z and Zhang Y (2020). Anesthesia and surgery induce age-dependent changes in behaviors and microbiota. Aging (Albany NY), 12(2):1965-86.

[46] Barnes CA (1979). Memory deficits associated with senescence: a neurophysiological and behavioral study in the rat. J Comp Physiol Psychol, 93(1):74-104.

[47] Nunes MA, Schöwe NM, Monteiro-Silva KC, Baraldi-Tornisielo T, Souza SI, Balthazar J, Albuquerque MS, Caetano AL, Viel TA and Buck HS (2015). Chronic Microdose Lithium Treatment Prevented Memory Loss and Neurohistopathological Changes in a Transgenic Mouse Model of Alzheimer's Disease. PLoS One, 10(11):e0142267.

[48] Lin D, Cao L, Wang Z, Li J, Washington JM and Zuo Z (2012). Lidocaine attenuates cognitive impairment after isoflurane anesthesia in old rats. Behav Brain Res, 228(2):319-27.

[49] Zhang J, Tan H, Jiang W and Zuo Z (2014). Amantadine alleviates postoperative cognitive dysfunction possibly by increasing glial cell line-derived neurotrophic factor in rats. Anesthesiology, 121(4):773-85.

[50] Yoder RM and Kirby SL (2014). Otoconia-deficient mice show selective spatial deficits. Hippocampus, 24(10):1169-77.

[51] Rosenfeld CS and Ferguson SA (2014). Barnes maze testing strategies with small and large rodent models. J Vis Exp, (84):e51194.

[52] Flinn JM, Bozzelli PL, Adlard PA and Railey AM (2014). Spatial memory deficits in a mouse model of late-onset Alzheimer's disease are caused by zinc supplementation and correlate with amyloid-beta levels. Front Aging Neurosci, 6:174.

[53] Kharasch Evan D, Hankins Douglas C and Cox K (1999). Clinical Isoflurane Metabolism by Cytochrome P450 2E1. Anesthesiology, 90(3):766-71.

[54] Tan X, Liu R, Dan L, Huang H and Duan C (2024). Effects of anesthetics on mitochondrial quality control: mechanisms and clinical implications. Anesthesiology and Perioperative Science, 2(3):31.

[55] Xie G, Cui Jn, Zhai Z and Zhang J (2020). Distribution characteristics of trifluoroacetic acid in the environments surrounding fluorochemical production plants in Jinan, China. Environ Sci Pollut Res, 27(1):983-91.

[56] Solomon KR, Velders GJ, Wilson SR, Madronich S, Longstreth J, Aucamp PJ and Bornman JF (2016). Sources, fates, toxicity, and risks of trifluoroacetic acid and its salts: Relevance to substances regulated under the Montreal and Kyoto Protocols. J Toxicol Environ Health B Crit Rev, 19(7):289-304.

[57] Dekant W and Dekant R (2023). Mammalian toxicity of trifluoroacetate and assessment of human health risks due to environmental exposures. Arch Toxicol, 97(4):1069-77.

[58] Sun C and Corbett B (2018). Trifluoroacetic acid: Three times the fluoride, three times the toxicity? Am J Emerg Med, 36(3):529.e1-.e2.

[59] Liu Y, Yu X, Han P, Chen X, Wang F, Lian X, Li J, Li R, Wang B, Xu C, Li J, Zheng Y, Zhang Z, et al. (2022). Gender-specific prevalence and risk factors of mild cognitive impairment among older adults in Chongming, Shanghai, China. Front Aging Neurosci, 14:900523.

[60] Levine DA, Gross AL, Briceño EM, Tilton N, Giordani BJ, Sussman JB, Hayward RA, Burke JF, Hingtgen S, Elkind MSV, Manly JJ, Gottesman RF, Gaskin DJ, et al. (2021). Sex Differences in Cognitive Decline Among US Adults. JAMA Netw Open, 4(2):e210169.

[61] Lin KA, Choudhury KR, Rathakrishnan BG, Marks DM, Petrella JR and Doraiswamy PM (2015). Marked gender differences in progression of mild cognitive impairment over 8 years. Alzheimers Dement (N Y), 1(2):103-10.

[62] Shaker B, Lee J, Lee Y, Yu M-S, Lee H-M, Lee E, Kang H-C, Oh K-S, Kim HW and Na D (2023). A machine learning-based quantitative model (LogBB_Pred) to predict the blood–brain barrier permeability (logBB value) of drug compounds. Bioinformatics, 39(10):btad577.